INCORPORATING EXPERT PRIOR KNOWLEDGE FOR ORAL LESION RECOGNITION

Anonymous authors
Paper under double-blind review

ABSTRACT

External information may improve predictive accuracy and uncertainty in medical image recognition. For example in oral lesion recognition, some lesion types are implausible to occur at certain anatomical locations. We propose a strategy to induce the prior knowledge about such correlations using an additional loss term that optimizes for plausible lesion types given an anatomical location. Our results suggests an improvement in model calibration, reduction in predicted number of implausible classes and improved uncertainty estimation for implausible predictions.

1 INTRODUCTION

Expert clinicians use prior knowledge on distribution of lesion types to diagnose oral lesions in addition to visual features of a case. One such crucial information is the anatomical location of the lesion. There are certain lesion types which rarely occur in certain anatomical locations. In limited data settings, the observed class distribution do not reflect the real-life distribution and thus the observed correlation structure between anatomical site and lesion type is biased. This leads a deep learning models to predict implausible classes, or never predict some lesions for some anatomical site.

The current work focuses on methods to incorporate expert knowledge about the correlation structure between anatomical locations and lesion types into the model. Specifically, the extreme case where certain lesion types are implausible to occur at certain anatomical locations (See Fig. 2 in appendix). Furthermore, we investigate the implication on the prediction uncertainty using approximate bayesian method, Monte Carlo DropConnect (MC-DropConnect) (Mobiny et al., 2021).

Contributions of this work is a general method to incorporate expert knowledge during training. The proposed method has been shown to effectively reduce the number of implausible predictions and improve different metrics compared to baseline method. Furthermore, our experiments demonstrate that the method yields better uncertainty estimates for implausible predictions.

2 METHOD

The MC-DropConnect setting approximates Bayesian inference by activating dropout and its variant DropConnect layers at training and inference time. As a result, a different subset θ_t of the network's weights are activated at each forward pass in the network and allows to sample the model posterior distribution for uncertainty quantification.

Given a dataset $\mathcal{D} = (\mathbf{x}, \mathbf{y})$ where $\mathbf{x}$ and $\mathbf{y}$ represent the input image and corresponding target vector, respectively. We define a neural network $\mathcal{M}$ that predicts output probabilities $\hat{\mathbf{y}} = \mathcal{M}_{\theta_t}(\mathbf{x})$. To account for anatomical constraints, we construct a set of implausible lesions ω given the anatomical site of the lesion present in the image based on the prior external knowledge shown in Fig. 2. To train the model, in addition to the cross-entropy loss (CE), we add a penalization term that computes mean squared error (MSE) between the output probabilities $\hat{\mathbf{y}}$ and one-hot encoded target-vector $\mathbf{y}$ only for implausible lesion types given in ω. The penalization term is defined as:

$$L_{MSE} = \frac{1}{N}\sum_{i=1}^{N}\sum_{c=1}^{C}(y_{i,c} - \hat{y}_{i,c})^2 * \mathbb{1}_{(c \in \omega_i)},$$

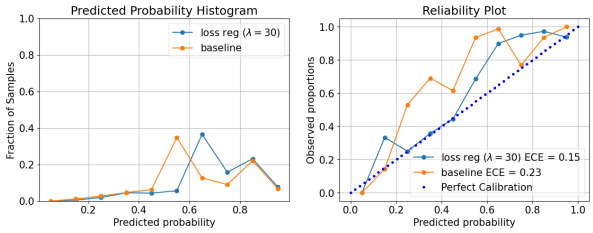

Figure 1: Reliability plot comparing our method and the baseline. The left panel is the confidence histogram, the right panel is the calibration curve along with Expected Calibration Error (ECE). We observe that ECE is substantially reduced for our method.

where C is the number of classes and N is the number of samples. We note that the set of implausible lesion ω changes per sample based on the anatomical location of the lesion. Finally, the loss function of our model can be written $L = L_{CE} + \lambda L_{MSE}$ where λ is the weight factor.

3 Experiments and Results

Dataset The dataset includes 2700 images featuring 16 distinct oral lesion types, each tagged with an anatomical location label. A matrix of plausible anatomical locations for each class was created by consulting with oral pathologists and literature shown in Fig. 2. It can be seen that most lesion types can occur at multiple anatomical sites, and three of them are linked to a unique anatomical site. Unfortunately, we have chosen not to release the dataset publicly due to privacy concerns.

Discussion of results Table1 shows a comparison between a baseline model and four versions of the proposed method with different loss weights $\lambda \in (5, 10, 30, 50)$. One hundred stochastic forward passes were considered to sample the model posterior and compute different metrics for each experiment. Implausible predictions represent the number of predictions of a lesion type incoherent with the anatomical site visible in the image. The number of implausible predictions is mainly decreased, and calibration is improved for high weights associated with the penalization term. Mutual information can be interpreted as a measure of model uncertainty, one should note the higher mutual information values for implausible predictions by our method compared to the baseline. It shows an improved quality of uncertainty estimation induced by the penalization term. Finally, Fig. 1 shows a significant improvement in the model calibration averaged over all the classes.

Table 1: Comparison of baseline and our methods with different values of λ. MI stands for Mutual Information, SBS for Scaled Brier Score and ECE stands for Expected Calibration Error. The details about different metrics can be found in Appendix A.4.

Methods	Implausible preds	MI for implausible preds	SBS	ECE
Baseline ($\lambda = 0$)	13/622	0.10	0.690	0.23
Ours ($\lambda = 5$)	11/622	**0.16**	0.696	0.19
Ours ($\lambda = 10$)	**8/622**	0.15	0.715	0.20
Ours ($\lambda = 30$)	11/622	0.13	**0.718**	**0.15**
Ours ($\lambda = 50$)	**8/622**	0.15	0.711	0.18

4 Conclusion

In this work, we presented a method to incorporate expert knowledge into deep learning models through penalization term. We demonstrate that it can improve model performance by decreasing the number of predictions incoherent with external domain knowledge. Additionally, our method seems to have a beneficial effect on the training by improving uncertainty estimation and calibration for oral lesion recognition task. This approach can be extended to other tasks where similar correlation structures are observed.

URM STATEMENT

The authors of this submission self-identify as members of an underrepresented minority. At least two authors are from a visible minority group, at least two authors are below 30 years of age, and two of the authors are first-time submitters to ICLR.

REFERENCES

Glenn W Brier et al. Verification of forecasts expressed in terms of probability. *Monthly weather review*, 78(1):1–3, 1950.

Jia Deng, Wei Dong, Richard Socher, Li-Jia Li, Kai Li, and Li Fei-Fei. Imagenet: A large-scale hierarchical image database. In *2009 IEEE Conference on Computer Vision and Pattern Recognition*, pp. 248–255, 2009. doi: 10.1109/CVPR.2009.5206848.

Aryan Mobiny, Pengyu Yuan, Supratik K Moulik, Naveen Garg, Carol C Wu, and Hien Van Nguyen. Dropconnect is effective in modeling uncertainty of bayesian deep networks. *Scientific reports*, 11(1):1–14, 2021.

Mingxing Tan and Quoc Le. Efficientnet: Rethinking model scaling for convolutional neural networks. In *International conference on machine learning*, pp. 6105–6114. PMLR, 2019.

A APPENDIX

A.1 DATA COLLECTION AND SPECIFICS

The dataset was collected by oral pathologists as part of the routine clinical examination of patients with oral lesions and is a part of their electronic health record. The images were captured using a digital camera of varying quality, under dental clinic lighting. The ground truth labels are obtained from pathology reports following the gold-standard diagnosis technique of biopsy or expert clinician's diagnosis. Due to the limitation of access to the oral cavity, images of specific anatomical locations (e.g. palate) can only be taken in a limited number of ways. Further, images may contain identifiable information about the patient (e.g., parts of eyes, skin color, dentition) and hence we, unfortunately, are not able to provide an open dataset. Our protocol was approved by Institutional Review Board.

Data leakage One of the key challenges in oral lesion classification is the issue of data leakage, which occurs when the algorithm learns by using information from the data that should not be used for the task at hand such as the shape of teeth etc. This can lead to overfitting and poor generalization of the model. To avoid data leakage, we created clusters of images such that the images of the same patient are kept in the same cluster. We make use of EXIF data from the images and other information such as patient names, lesion types, and anatomical sites to make clusters of images. We assign these clusters to either training or test sets to avoid data leakage.

A.2 CONSTRUCTION OF EXPERT KNOWLEDGE MATRIX OF IMPLAUSIBLE LESIONS (ω_i)

An initial matrix was constructed after a comprehensive review of the literature on the reported occurrence of each type of oral lesion. The literature included peer-reviewed publications, pedagogical textbooks, and other reports. This initial matrix was reviewed for correctness and completeness by oral pathology experts. The final matrix is presented in Fig. 2. For each training and test sample, the column of this matrix corresponding to the anatomical location of the lesion in the image is chosen as the ω_i.

A.3 TRAINING DETAILS

For all our experiments, we use an ImageNet Deng et al. (2009) pretrained efficientnet-b5 Tan & Le (2019). We finetune the full network weights for 400 epochs using RMSprop optimizer with an initial learning rate of 10^{-3}. We use a dropout and dropconnect rate of 0.5.

A.4 METRICS

Brier score (Brier et al., 1950) is equivalent to a MSE between the predicted vector and the one-hot encoded ground truth. The Scaled Brier Score (SBS) is a skill score that allows comparison with a reference Brier score (BS_{ref}) such as $SBS = 1 - \frac{BS}{BS_{ref}}$. The reference was chosen to be a non-informative model that outputs the marginal proportion of classes for every sample. Scaled Brier score has the added advantage that it is not affected by the marginal distribution of the true class.

Expected Calibration Error: Evaluating calibration consists of measuring the statistical consistency between the predictive distribution and the observed proportion *i.e.* the accuracy of the predictive distribution. Expected Calibration Error is a binning methods where the predictive probability y_{pred_i} is computed and grouped into M bins $b_1, ..., b_M$. Then, calibration of the single bins is evaluated by setting the average bin predictive probability :

$$pp(b_m) = \frac{1}{|b_m|} \sum_{s \in b_m} y_{pred_s}$$

in relation with the observed proportions:

$$op(b_m) = \frac{1}{|b_m|} \sum_{s \in b_m} \mathbb{1}(\arg\max(y_{pred_s}) = \arg\max(y_s))$$

The model is calibrated when $pp(b_m) = op(b_m)$, the Expected Calibration Error gives a quantitative evaluation define by:

$$ECE = \sum_{m=1}^{M} \frac{|b_m|}{N} |pp(b_m) - op(bm)|$$

Mutual Information (MI) is defined by the amount of information gained about the model parameters by receiving a test sample $\mathbf{x}$ and its corresponding true label $\mathbf{y}$.

$$I(\mathbf{y}, \theta | \mathbf{x}, \mathcal{D}) = H(\mathbf{y}|\mathbf{x}, \mathcal{D}) - \mathbb{E}_{p(\theta|\mathcal{D})} H(p(\mathbf{y}|\mathbf{x}, \theta))$$

where H is the predictive entropy that can be approximated by Bayesian approximation using Monte Carlo sampling

$$H(\mathbf{y}|\mathbf{x}, \mathcal{D}) = -\sum_c p(\mathbf{y} = c|\mathbf{x}, \mathcal{D}) \log p(\mathbf{y} = c|\mathbf{x}, \mathcal{D}) \approx -\sum_c p_{MC}(\mathbf{y} = c|\mathbf{x}) \log p_{MC}(\mathbf{y} = c|\mathbf{x})$$

where p_{MC} is the average of the predictive probability over T Monte Carlo forward passes. It yields

$$I(\mathbf{y}, \theta | \mathbf{x}, \mathcal{D}) \approx H(\mathbf{y}|\mathbf{x}, \mathcal{D}) - \sum_c \frac{1}{T} \sum_{t=1}^{T} p(\mathbf{y} = c|\mathbf{x}, \theta_t) \log p(\mathbf{y} = c|\mathbf{x}, \theta_t)$$

A.5 ADDITIONAL RESULTS

We show reliability plots for each anatomical site in Fig. 3 to 10. We observe that the expected calibration error (ECE) is decreased for almost all anatomical sites except retromolar trigone as shown in Fig. 9. It is known that ECE is sensible to the number of samples considered, which is low for retromolar trigone location.

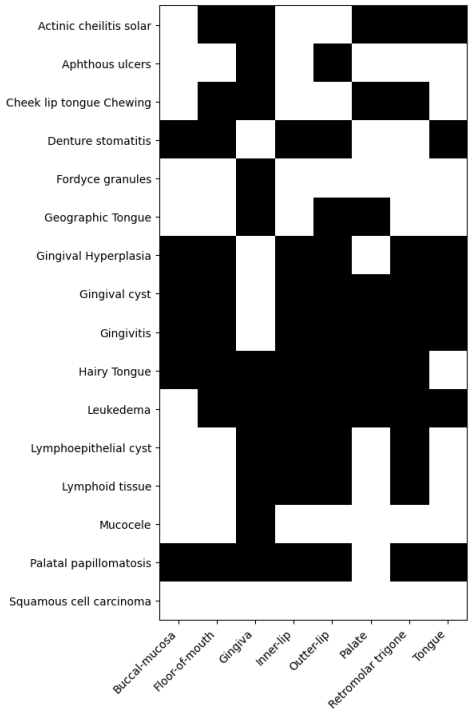

Figure 2: Anatomical site and lesion occurrence plausibility. Black square represents implausibility of the lesion type to occur on the anatomical site. White square represents plausibility.

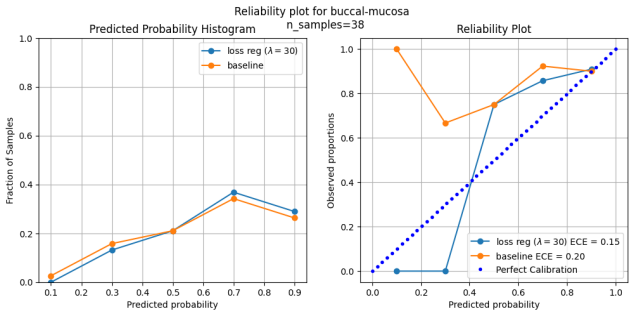

Figure 3: Reliability plot for buccal-mucosa anatomical site.

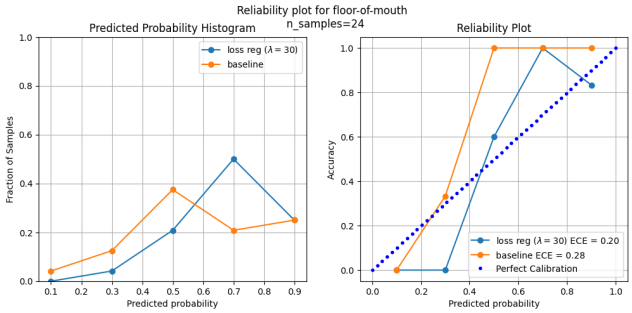

Figure 4: Reliability plot for floor of mouth anatomical site.

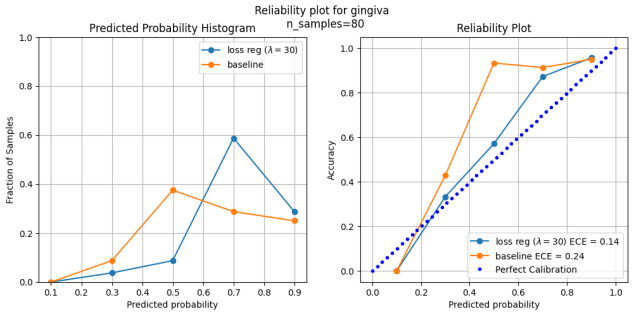

Figure 5: Reliability plot for gingiva anatomical site.

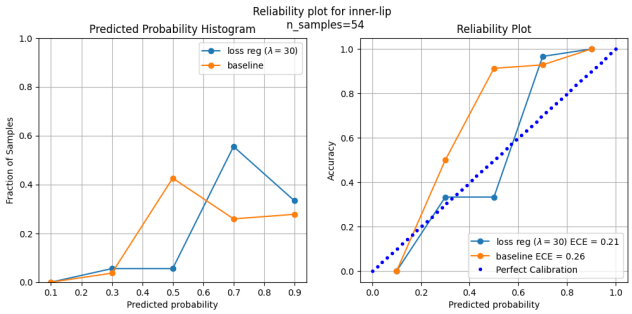

Figure 6: Reliability plot for inner-lip anatomical site.

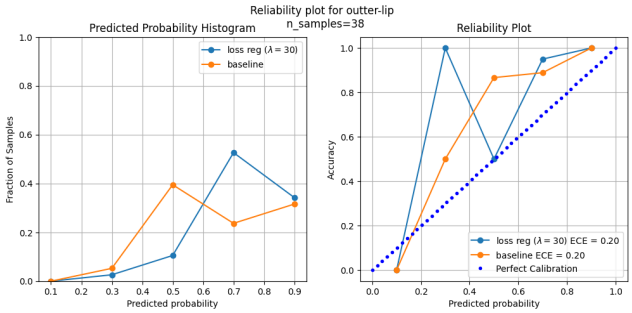

Figure 7: Reliability plot for outter-lip anatomical site.

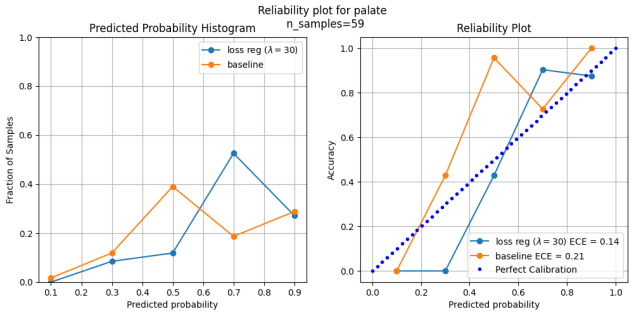

Figure 8: Reliability plot for palate anatomical site.

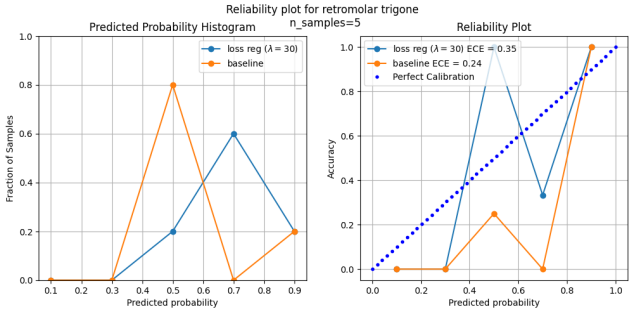

Figure 9: Reliability plot for retromolar trigone anatomical site.

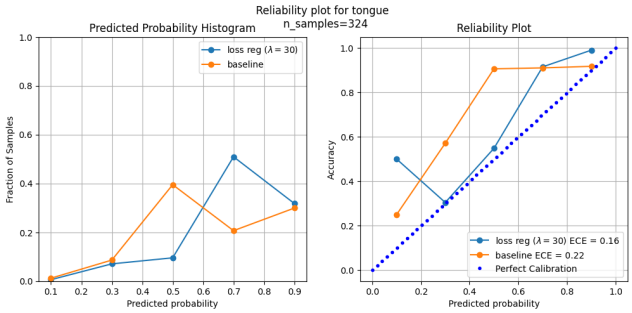

Figure 10: Reliability plot for tongue anatomical site.